

Caspase 3 Inactivation Protects Against Hepatic Cell Death and Ameliorates Fibrogenesis in a Diet-Induced NASH Model

Samjhana Thapaliya · Alexander Wree · Davide Povero ·
Maria Eugenia Inzaugarat · Michael Berk · Laura Dixon ·
Bettina G. Papouchado · Ariel E. Feldstein

Received: 25 February 2014 / Accepted: 12 April 2014 / Published online: 3 May 2014
© Springer Science+Business Media New York 2014

Abstract

Background/Aims Hepatocyte cell death is a key feature of nonalcoholic steatohepatitis (NASH). As the contribution of specific caspases remains unclear, our aim was to ascertain the effect of caspase 3 suppression on liver injury and fibrogenesis.

Methods C57BL/6 wild-type (WT) and caspase 3 knock out (*Casp3*^{-/-}) mice were placed on a methionine- and choline-deficient (MCD) diet for 6 weeks to induce steatohepatitis and liver fibrosis. Thereafter, liver injury, liver fibrosis and hepatocellular apoptosis were quantified in liver sections. Additionally, expression of proteins associated with liver inflammation and fibrogenesis was analyzed.

Results WT mice fed MCD diet showed marked activation of caspase 3 in hepatocytes, in conjunction with steatohepatitis and increased hepatic triglyceride levels, hepatocyte ballooning, inflammation and fibrosis.

Casp3^{-/-} mice fed the MCD diet showed similar serum aminotransferase levels and NAFLD activity scores (NAS) compared with WT MCD-fed mice. However, *Casp3*^{-/-} mice on the MCD diet showed a marked reduction in expression of transcripts for profibrogenic genes, which translated into reduced hepatic collagen deposition. These changes were associated with decreased levels of apoptosis, and a significant reduction in the expression of cytokines involved in inflammatory signaling. *Casp3*^{-/-} mice on the MCD showed a reduction in expression of chemokine receptor 2 (CCR2) leading to ameliorated infiltration of inflammatory lymphocyte antigen 6 complex, locus C1 (Ly6c) positive monocytes.

Conclusion These findings support a prominent role for hepatocyte caspase 3 activation in NASH-related apoptosis, fibrogenesis and fibrosis which in part is mediated via CCR2-dependent infiltration of Ly6c positive monocytes.

Keywords Nonalcoholic fatty liver disease · Caspases · Apoptosis · Liver injury · Liver fibrosis

Samjhana Thapaliya and Alexander Wree have contributed equally to this work.

Electronic supplementary material The online version of this article (doi:10.1007/s10620-014-3167-6) contains supplementary material, which is available to authorized users.

S. Thapaliya · M. Berk · L. Dixon
Department of Cellular and Molecular Medicine, Lerner
Research Institute, Cleveland Clinic, Cleveland, OH, USA

A. Wree · D. Povero · M. E. Inzaugarat · A. E. Feldstein (✉)
Department of Pediatrics, University of California, San Diego,
9500 Gilman Drive, MC 0715, La Jolla, CA 92037-0715, USA
e-mail: afeldstein@ucsd.edu

B. G. Papouchado
Department of Pathology, University of California, San Diego,
La Jolla, CA, USA

Introduction

Nonalcoholic fatty liver disease (NAFLD) is currently the most common form of chronic liver disease in the Western world affecting both adults and children and is strongly associated with obesity and insulin resistance [1, 2]. Hepatic steatosis, a stage within the spectrum of NAFLD, characterized by triglyceride accumulation in liver cells and follows a benign nonprogressive clinical course, is present in one out of three adults and one in ten children or adolescents in the USA [3, 4]. Some patients exhibit lipid accumulation with evidence of cellular damage, inflammation and different degrees of scarring or fibrosis which is

commonly referred as nonalcoholic steatohepatitis (NASH) [5]. Several studies have shown that NASH is a serious condition with approximately 25 % of affected patients progressing to cirrhosis and being in danger of its associated complications: portal hypertension, liver failure and hepatocellular carcinoma [6–8].

Since the original description that caspase activation and apoptotic cell death are characteristic pathologic features in the liver of NASH patients [9], increasing amount of data have demonstrated that hepatocyte cell death is a key process involved in NASH pathogenesis [10]. Caspases belong to a family of highly conserved cysteine-dependent aspartate-specific acid proteases that use a cysteine residue as catalytic nucleophile and share a stringent specificity for cleaving their substrates after aspartic acid residues in target proteins [11]. They are synthesized as inert zymogens and upon receipt of apoptotic stimuli, cells activate initiator caspases such as, caspase-1, -2, -8, -9 and -10 that, in turn, proteolytically cleave and activate effector caspases including caspase-3, -6 and -7 [12]. Caspases have been further categorized as either proinflammatory or proapoptotic, depending upon their participation in these cellular responses. Caspase 3, the prototype of a prodeath caspase, plays a central role in the apoptotic machinery [13]. In this process, caspase 3 recognizes four contiguous amino acids (designated P4–P3–P2–P1–P1′) and cleaves the peptide bond between the P1–P1′ residues [14, 15].

The relative contribution of proapoptotic versus proinflammatory caspases to liver pathology during NASH development, as well as in the protective effects of pan-caspase inhibitors, remains incompletely understood. Given its central role in apoptosis, blocking caspase activity is now widely used as a therapeutic and diagnostic approach for several diseases, including NASH [16–19]. Recent studies have demonstrated that pan-caspase inhibition prevents the development of steatohepatitis [20–22]. Taking into account that caspase 3 has been identified to be the main player of apoptotic cell death, we examined the effects of selective inactivation of caspase 3 during progression of steatohepatitis and fibrosis in vivo, and the cross talk between hepatocytes and hepatic stellate cells (HSC) in vitro during lipotoxicity.

Methods

Animal Studies

The experimental protocols were approved by the Institutional Animal Care and Use Committee at the Cleveland Clinic. Caspase 3 knockout mice (*Casp3*^{-/-}) were generously provided by Dr. Mina Woo (University of Toronto). These mice were generated by deleting exon 3 of the

CPP32/caspase 3 gene as previously described in detail [20]. They appear healthy and do not have a particular phenotype, but they do have a slight decrease in life span. *Casp3*^{-/-} mice and their wild-type controls, 20–25 g of body weight, 7 weeks old, were placed on a methionine- and choline-deficient (MCD) diet (TD 90262, Teklad Mills, Madison, WI), which has been extensively shown to result in steatosis associated with significant inflammation and progressive fibrosis pathologically similar to human severe steatohepatitis [21, 22] or a control diet (CTL) consisting of 5 % fat (TD 2918, Teklad Mills, Madison, WI) to act as controls ($n = 4–6$ in each group). Animals in each group were killed after 6 weeks on the respective diets, and their liver tissue and plasma were collected under deep anesthesia as previously described in detail [16].

Histopathology, Immunohistochemistry, and Serum Assays

Liver tissue was fixed in 4 % paraformaldehyde and embedded in Tissue Path (Fisher Scientific, Pittsburgh, PA, USA). Tissue sections (4 μm) were prepared, and hematoxylin and eosin, as well as Oil Red O-stained liver specimens were evaluated by light microscopy. Individual features including degree of steatosis, inflammation and ballooning were assessed in MCD and CTL-fed animals by an experienced pathologist (BGP) in a blinded fashion. Steatosis, inflammation and ballooning were scored based on NAFLD activity score [23]. Serum alanine aminotransferase (ALT) determinations were performed using a commercial kit (Sigma Diagnostics, St. Louis, MO, USA). Liver triglycerides were quantified using a specific kit following manufacturer's instructions (Pointe Scientific, Canton, MI, USA). Immunohistochemistry for hepatic macrophages (F4/80, AbD Serotec, Raleigh, NC, USA) was performed in formalin-fixed, paraffin-embedded livers according to manufacturer's instructions. Immunohistochemistry for lymphocyte antigen 6 complex, locus C1 (Ly6c) (Abcam, Cambridge, MA, USA) was performed on frozen liver sections.

Apoptosis and Caspase 3 Assessment

Terminal deoxynucleotidyl transferase dUTP nick end labeling (TUNEL) assay was performed following manufacturer's instructions (in situ cell death detection kit; Roche Molecular Biochemicals, Mannheim, Germany). Hepatocyte apoptosis in liver sections was quantified by counting the number of TUNEL-positive cells in five random microscopic fields (40×), as previously described [28]. Caspase activation was quantified using biochemical and immunohistochemical techniques: Caspase-Glo 3/7 Assay (Promega, Madison, WI, USA); immunostaining for

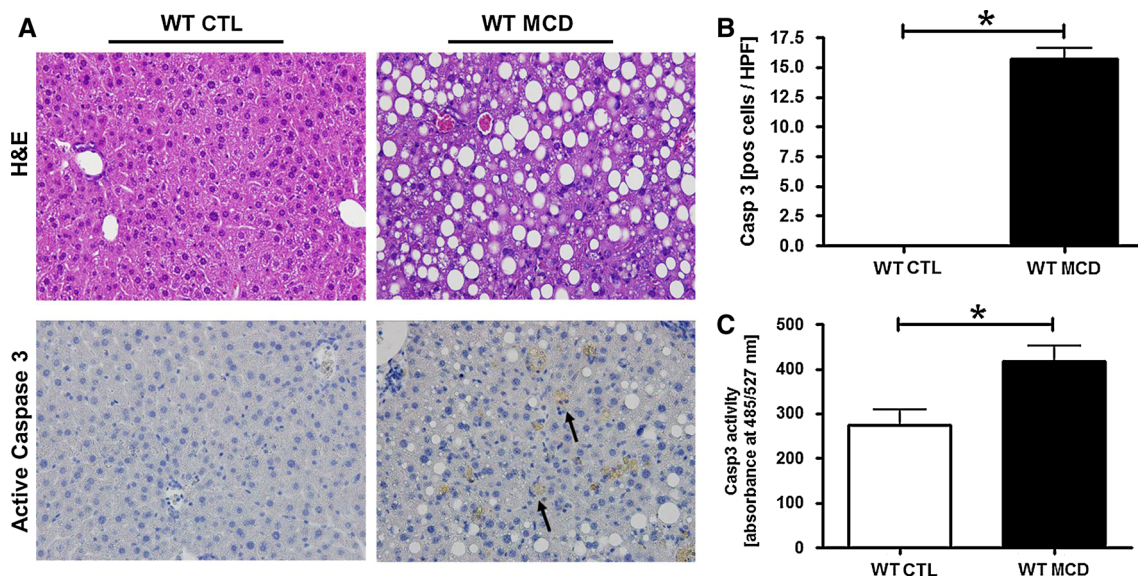


Fig. 1 MCD diet results in steatohepatitis development and marked hepatocyte caspase 3 activation. **a** Representative pictures of Hematoxylin & Eosin (H&E) staining and active caspase 3 immunohistochemistry of liver from the wild-type animals on the MCD or control

diets (magnification $\times 40$) and corresponding quantification (**b**). **c** Caspase 3 activation in the different groups of mice was assessed by Apo-ONE Homogeneous Caspase 3 fluorometric assays. Results are represented as mean \pm SEM. * $P < 0.05$

active caspase 3 was performed using an antibody specific for the detection of cleaved caspase 3 (Cell Signaling, Boston, MA, USA).

Determination of Liver Fibrosis

Liver fibrosis was assessed using Sirius red staining and α -smooth muscle actin (α -SMA) immunofluorescence. Direct Red 80 and Fast Green FCF (color index 42053) were provided by Sigma-Aldrich. Liver sections were incubated in the dark for 2 h at room temperature with an aqueous solution of saturated picric acid containing 0.1 % Direct Red. Stained slides were washed slowly under running distilled water for 6 min, dehydrated (3 min for each step), mounted and examined by light microscopy. Red-stained collagen fibers were quantitated by digital image analysis. Immunofluorescence for α -SMA (Sigma) was performed on paraffin-embedded liver tissue using standard DAB technique (Vector, Burlingame, CA, USA) following manufacturer's instructions.

Real-Time PCR

Total RNA was isolated from liver tissue using RNeasy Lipid Tissue Mini kit (Qiagen, Valencia, CA). Reverse transcript (the cDNA) was synthesized from 1 μ g total RNA using iScript cDNA Synthesis Kit (Bio-Rad, Hercules, CA). Real-time PCR quantification was performed. Briefly, 25 μ l reaction mix contained: cDNA, SYBR Green buffer, Gold Taq polymerase, dNTPs and primers at final

concentration of 200 μ M. Primer sequences used for quantitative PCR are given in supplementary table 1. RT-PCR was performed in the Mx3000P cycler (Stratagene): 95 $^{\circ}$ C for 10 min, 40 cycles of 15 s at 95 $^{\circ}$ C, 30 s at 60 $^{\circ}$ C, 30 s at 72 $^{\circ}$ C followed by a 1 min at 95 $^{\circ}$ C, 30 s at 55 $^{\circ}$ C and 30 s at 95 $^{\circ}$ C. The fold change over control samples was calculated using CT, Δ CT and $\Delta\Delta$ CT values using MxPro software (Stratagene). 18S ribosomal RNA (Ambion Inc, Austin, TX) was used as an endogenous control.

Western Blot

For immunoblot analysis, 30 mg whole liver lysate was resolved by a 4–20 % gradient gel, transferred to nitrocellulose membrane and blotted with an anti- α -SMA (GeneTex, Irvine, CA, USA) antibody. Membranes were incubated with peroxidase-conjugated secondary antibody (dilution 1:10,000) (GeneTex, Irvine, CA, USA); protein bands were visualized with the enhanced chemiluminescence reagent and digitized using a CCD camera (Chemi-Doc[®], Biorad, Hercules, CA, USA). Expression intensity was quantified by ImageLab (Biorad). Protein load was verified with an α -tubulin antibody (dilution 1:10,000) (Hybridomabank, University of Iowa).

Statistical Analysis

Analyses were performed with Graph Pad (version 5.03; Graph Pad, Graph Pad Software Inc., CA, USA). Unless otherwise stated, data are expressed as mean \pm SEM or as

absolute number or percentage for categorical variables. Differences between groups were compared by ANOVA followed by a post hoc Bonferroni test to correct for multiple comparisons. Differences were considered to be statistically significant at $P < 0.05$.

Results

Caspase 3 Activation Is a Prominent Pathological Feature in Experimental NASH

To investigate the role of caspase activation in the pathogenesis of NASH, we initially placed C57BL/6 mice on the methionine- and choline-deficient (MCD) diet which has been extensively shown to be associated with progressive fibrosing steatohepatitis pathologically similar to human severe steatohepatitis [21, 22]. After 6 weeks on the

respective diets, we observed significant hepatic fat accumulation induced by MCD feeding (Fig. 1a), in conjunction with an increase in histological parameters of liver injury including hepatic inflammation and hepatocyte ballooning. These changes were associated with a marked increase in the expression of cleaved caspase 3 which was primarily localized to hepatocytes showing a predominantly cytoplasmic staining pattern (Fig. 1a, b). The changes observed in the level of cleaved caspase 3 were accompanied by a significant increase in hepatic caspase 3 activity (Fig. 1c).

Caspase 3 Suppression Is Associated with Decreased Hepatocellular Damage, Cell Death, and Proinflammatory Signaling

Having established the presence of increased caspase activity in the liver of MCD-fed mice, we next sought to

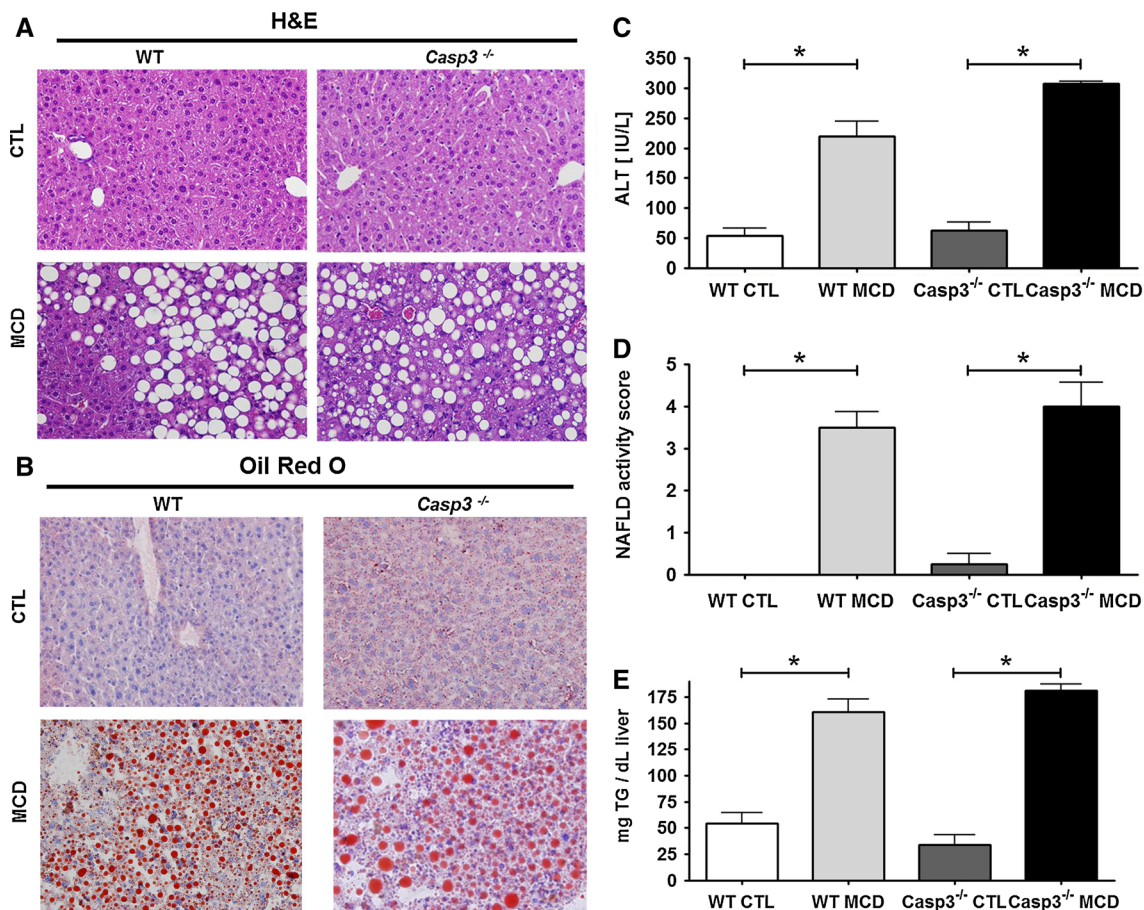


Fig. 2 Metabolic changes, histological features, hepatic triglyceride levels and serum ALT levels in *Casp3*^{-/-} and WT mice on the MCD and CTL diets. Male C57BL/6 mice (wild type), 20–25 g of body weight and C57BL/6 caspase 3 knockout (*Casp3*^{-/-}) were placed on either a control diet or methionine- and choline-deficient (MCD) diet for 6 weeks. Histological microphotographs of Hematoxylin & Eosin (H&E) and (a) Oil red O-stained liver sections of animals from the four

different groups of mice (b) (magnification $\times 40$). Serum ALT levels assessed at the time of killing showed significantly increased level in mice fed with MCD regardless of the genetic background (c). NAFLD activity score also showed significantly increased level in mice fed with the methionine deficient diet (d) Hepatic triglyceride levels was assessed in all mice at the time of killing and the mean \pm SEM are graphed (e). Results are represented as mean \pm SEM. * $P < 0.05$

investigate the role of caspase 3 during NASH development by using caspase 3 knockout mice (*Casp3*^{-/-}). We first investigated whether *Casp3*^{-/-} mice are resistant to liver injury and inflammation. C57BL/6 wild-type and *Casp3*^{-/-} mice were placed on either a MCD diet, or control (CTL) diet ($n = 5$ in each group) for 6 weeks. Wild-type mice on MCD diet developed the full spectrum of NASH with steatosis, inflammation, hepatocellular ballooning, resulting in an average NAFLD activity score (NAS) of 4 (Fig. 2a, d). Serum ALT levels were about fourfold higher in WT and *Casp3*^{-/-} mice on the MCD diet compared with animals fed the control diet (Fig. 2c). Microscopic examination showed that WT mice developed significant predominantly macro vesicular steatosis and no change in knockout mice compared with WT on MCD diet (Fig. 2b). Consistent with these results, hepatic triglyceride levels were similarly increased in both knockout and WT mice on the MCD diet compared with the control diet (Fig. 2e). We next quantified the amount of hepatocellular cell death present in the various groups of mice. Consistent with the significant caspase 3 activation found in the WT animals on the MCD diet, we observed increased TUNEL-positive cells in these mice, but not in the livers of *Casp3*^{-/-} mice fed the same diet (Fig. 3a, b).

Dietary-Induced Ly6c Positive Monocyte Infiltration Is Ameliorated in *Casp3*^{-/-} Mice

When we examined the inflammatory state of the liver at the molecular and cellular level, we found that the total number of Kupffer cells/macrophages (F4/80) and mRNA

expression levels were comparable in both groups of animals on the MCD diet (Fig. 4a, b). However, only wild-type mice on MCD diet, and not *Casp3*^{-/-} mice, showed a significant increase in number and mRNA expression level of inflammatory lymphocyte antigen 6 complex, locus C1 (Ly6c) positive monocytes (Fig. 4c, d). We also found that the major mediator of Ly6c infiltration—the chemokine receptor 2 (CCR2)—was significantly increased in WT mice on MCD diet when compared to WT mice on control diet and those levels were also significantly greater than those of *Casp3*^{-/-} mice on MCD diet (Fig. 4e). Analysis of markers for M1/M2 macrophage polarization (M1: TNF- α and IL-6; M2: Arg1 and IL-10) revealed a marked reduction in mRNA levels of TNF- α and IL-6 in the MCD-fed *Casp3*^{-/-} mice compared with the WT animals on the MCD diet (Fig. 4f). The same pattern was observed in the analysis of arginase 1 (Arg1), while mRNA levels of IL10 were increased in both groups fed with MCD diet without significant difference (Fig. 4g).

Hepatic Stellate Cell (HSC) Activation and Collagen Deposition from MCD Diet are Prevented by Caspase 3 Suppression

The differential findings observed in the *Casp3*^{-/-} mice in several aspects of hepatocyte viability and inflammatory signaling, two events that have been linked to HSC activation, led us to further examine the role of caspase 3 in fibrogenesis and fibrosis induced by the MCD diet. While after 6 weeks on the MCD diet, wild-type animals showed an almost fourfold increase in collagen deposition as

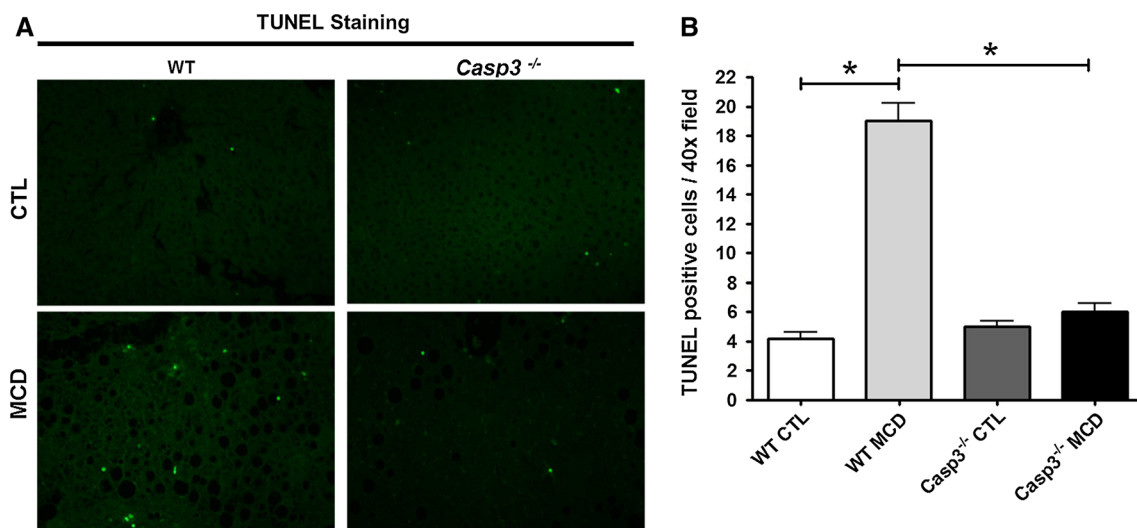
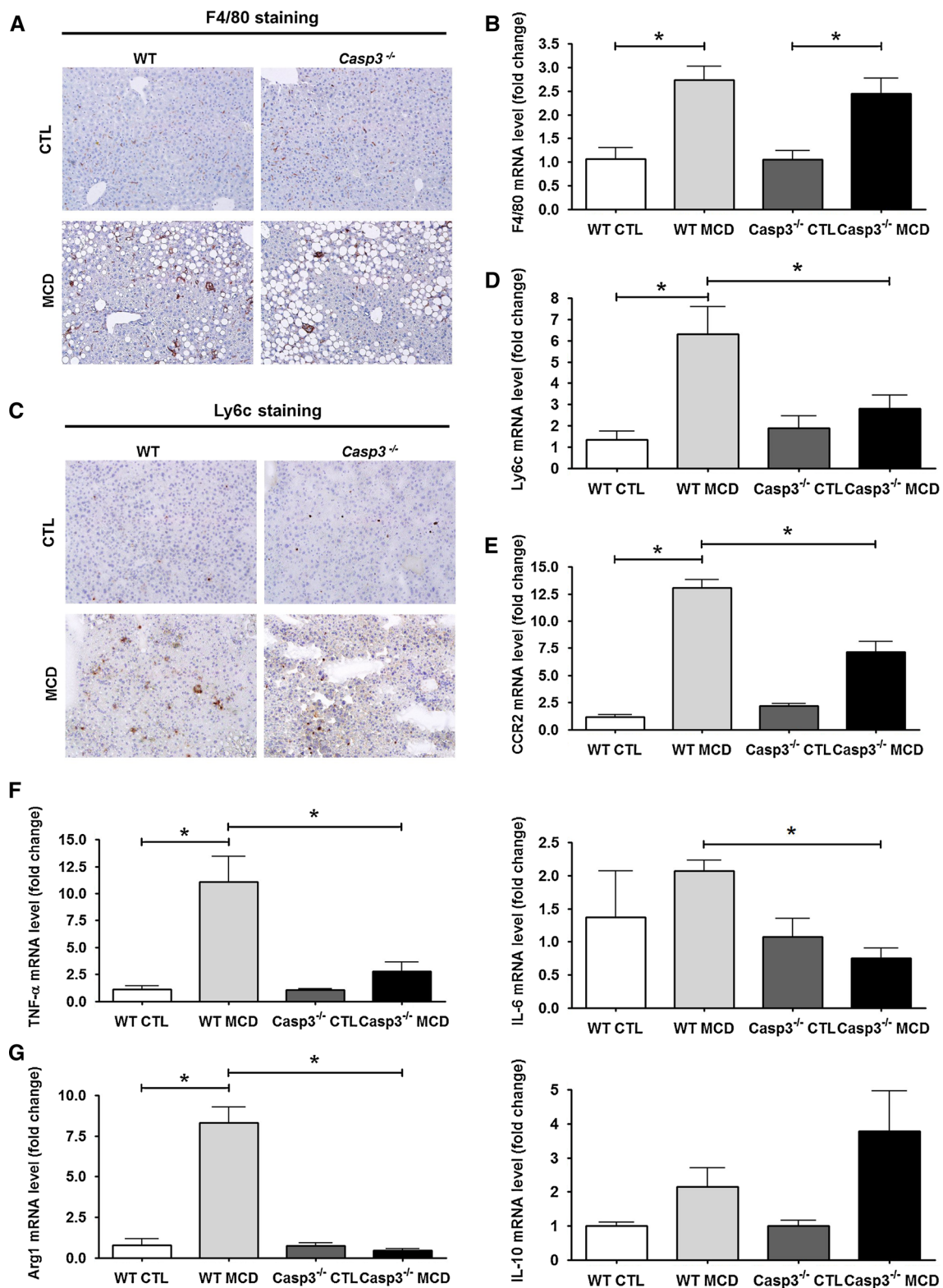


Fig. 3 Hepatocyte cell death is decreased in *Casp3*^{-/-} mice compared with WT mice on MCD diet. Tissues were fixed in 4 % paraformaldehyde and embedded in Tissue Path. Tissue sections (4 μ m) were prepared. **a** Representative images of Terminal deoxynucleotidyl transferase dUTP nick end labeling (TUNEL) staining in the four

groups of mice (magnification $\times 40$). **b** Semi-quantification of TUNEL-positive cells in *Casp3*^{-/-} mice and WT mice on MCD diet normalized to CTL diet. Results are represented as mean \pm SEM. * $P < 0.05$



demonstrated by Sirius red staining of liver tissue coupled to quantitation by digitized image analysis when compared to the wild-type animals on the control diet (Fig. 5a, b);

these changes were completely blunted in the Casp3^{-/-} mice (Fig. 5a, b). Similarly, an increase level of α -SMA protein expression was detected by both Western blot

Fig. 4 *Casp3*^{-/-} mice exhibit less Ly6c positive monocytes when compared to WT mice on MCD diet. The total number of Kupffer cells/macrophages (F4/80) (representative sections are shown in $\times 20$ magnification) and mRNA expression level were comparable in both groups of animals on the MCD diet (**a, b**) and significantly greater when compared to mice on control diet. Expression levels and number of inflammatory lymphocyte antigen 6 complex, locus C1 (Ly6c) positive monocytes (representative sections are shown in $\times 20$ magnification) was only found to be increased in wild-type mice on MCD diet and not *Casp3*^{-/-} (**c, d**). Expression of chemokine receptor 2 (CCR2) was significantly increased in WT mice on MCD diet when compared to WT mice on control diet, and those levels were also significantly greater than those of *Casp3*^{-/-} mice on MCD diet (**e**). mRNA levels of TNF- α and IL-6 were significantly reduced in MCD-fed *Casp3*^{-/-} mice when compared to WT mice on the MCD diet (**f**). Expression levels of Arg1 followed the same pattern, whereas mRNA levels of IL10 were increased in both groups fed with MCD diet without significant difference (**g**). Results are represented as mean \pm SEM. * $P < 0.05$

analysis and immunofluorescence in WT MCD-fed mice but not in *Casp3*^{-/-} MCD-fed mice compared with the animals on the control diet (Fig. 5c, d). In line with this, we also found that after 6 weeks on the MCD diet wild-type animals showed a marked increase in the mRNA expression of various genes involved in HSC activation and fibrogenesis (Fig. 5e). mRNA levels of COL1A1, α -SMA and TGF β all were increased in MCD-fed WT mice but were completely blunted in *Casp3*^{-/-} mice on the same diet (Fig. 5e). Taken together, these observations suggest that during NASH development, caspase 3 activity plays a central role in liver injury, and hepatic fibrosis.

Discussion

The principal findings of this study relate to the effects of specific caspase 3 activation during NASH development. Active caspase 3 was found to be more abundant in livers of WT mice fed with a dietary NASH model (MCD). Suppression of caspase 3 resulted in protection of hepatocellular damage, cell death and proinflammatory signaling. Notably, the recruitment of profibrotic inflammatory monocytes was ameliorated in caspase 3 knockout mice. This translated to a marked reduction in collagen deposition and development of liver fibrosis. Effects were found to be independent of hepatic triglyceride accumulation. The results of the current study demonstrate that caspase 3 activation in hepatocytes plays a central role in steatohepatitis and fibrosis.

The importance of caspase activation and hepatocytes undergoing apoptosis in the liver of NASH patients was described more than a decade ago [9]. Since then a growing number of studies have demonstrated that hepatocyte cell death is a key process involved in NASH pathogenesis [10]. Previous studies showed that both fundamental pathways of apoptosis, the so called extrinsic (death

receptor mediated) pathway and the intrinsic (organelle-initiated) pathway contribute to the development of NASH in mice [24, 25]. Although the relative importance or predominance of these two pathways in human NASH remains to be elucidated, in hepatocytes, both tend to converge at the level of the mitochondria resulting in permeabilization of the mitochondrial outer membrane and release of multiple proteins from the mitochondrial intermembrane space into the cytosol [26–28].

A central consequence of this process is the activation of the effector caspases (mainly caspase 3) which will then cleave a number of different substrates inside the cell resulting in the characteristic morphologic changes of apoptosis [29, 30]. Targeting caspase activity has gained significant attention for development of both novel therapeutic and diagnostic strategies for NASH patients. Three independent pre-clinical studies using different models of dietary-induced NASH in mice showed significant protective effects of pan-caspase inhibitors in both parameters of inflammation as well as fibrosis [31–33].

A key extant question is whether suppression of the effector caspase 3 in NASH would result in a switch to caspase 3-independent cell death, and thus, no protection or even worsening of liver disease by inducing a compensatory increase in necrotic cell death may occur. Our study demonstrates that caspase 3 suppression does not improve steatosis, histological inflammatory score parameters or decrease serum ALT levels in this mouse model of NASH. However, MCD-fed *Casp3*^{-/-} mice showed a reduction in indices of hepatocellular damage such as ballooning of hepatocytes, decreased level of apoptosis, marked decrease in proinflammatory signaling and reduced infiltration of inflammatory macrophages. Although based on observations in developing animals, and in vitro studies in immortalized cell lines, apoptosis has been perceived to be noninflammatory, it has become apparent that a pathological increase in apoptosis in the context of chronic diseases may directly or indirectly promote inflammation [34, 35]. The current data extend these observations and demonstrate that the protection from hepatocyte apoptosis seen in caspase 3 knockout mice was associated with a marked decrease in proinflammatory cytokines levels in liver tissue and infiltration of Ly6c inflammatory monocytes. It is known that sustained inflammation with chronic liver injury mainly induces the development of liver fibrosis with recent studies showing that liver-resident macrophages only partially conducted these actions, but this largely depends on the recruitment of monocytes into the liver [36–38]. Upon organ injury, chemokine receptor CCR2 promotes monocyte subset accumulation in the liver, namely of the inflammatory Ly6C+ (Gr1+) monocyte subset as precursors of tissue macrophages [39, 40]. In the present study, we were able to show that MCD induced

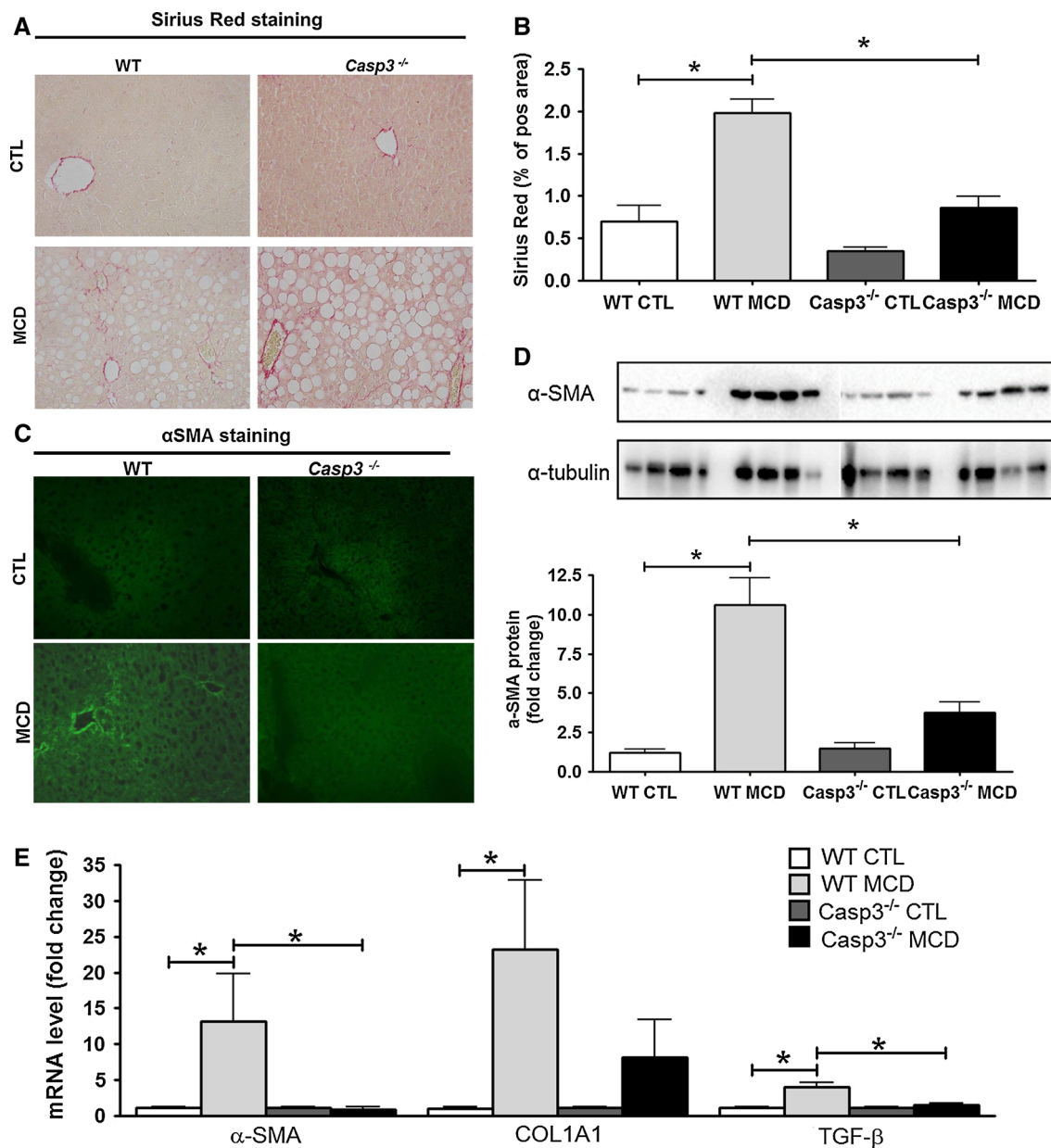


Fig. 5 Markers of HSC activation and collagen deposition are markedly decreased in *Casp3*^{-/-} mice compared with WT mice on MCD diet. Quantification of collagen fibers was performed in liver section stained with *Sirius red* (a) (magnification $\times 40$) and quantified using the surface area stained per field area \pm SD ($n = 4-6$ in each group) excluding blood vessels (b). Immunofluorescence staining of α -SMA was also performed on frozen liver section (c). α -SMA was detected using western blot assay from liver homogenates and

densitometry analysis of α -SMA over α -tubulin was analyzed (d). Quantitative RT-PCR analysis of HSC activation markers alpha-smooth muscle actin (α -SMA), collagen, type I-alpha (COL1A1), and transforming growth factor-beta (TGF- β) mRNA expression was assessed in WT and *Casp3*^{-/-} mice on the CTL and MCD diet ($n = 4-5$ in each group). Results are expressed as mean \pm SEM. * P value < 0.05

increase in CCR2 expression and recruitment of Ly6c positive macrophages is ameliorated in *Casp3*^{-/-} mice.

Another important aspect of blocking caspase 3 activation is the fact that this protease might be required for apoptosis of activated HSC which has been proposed as a potential mechanism to limit fibrogenesis, and thus, inhibition of such a process could hypothetically result in

fibrosis progression. As expected after 6 weeks on the MCD diet wild-type animals showed a marked increase in the expression of various genes involved in HSC activation and fibrogenesis, these changes were significantly reduced in the *Casp3*^{-/-} mice. More importantly, an almost four-fold increase in collagen deposition was present in wild-type animals on the MCD diet, and these changes were

completely blunted in the Casp3^{-/-} mice. The results of the current study suggest that inhibiting caspase 3 activation in hepatocytes significantly impacts the production of proinflammatory cytokines such as TNF- α and IL-6 and prevents HSC activation and fibrosis development. Moreover, these results support the concept that caspase 3 activation in parenchymal cells is a key stimulus for HSC activation and fibrosis and overpowers the potential fibrotic effects of caspase 3-independent cell death as well as the putative anti-fibrotic effect of HSC apoptosis induction. Future studies such as those using cell-type-specific caspase 3 knockout mice will be required to further dissect the role of caspase 3 activation in hepatocyte versus nonparenchymal cells of the liver in vivo and their potential distinct role in the pathophysiologic changes observed during NASH development. In summary, the current studies uncover the role of hepatic caspase 3 activation in experimental NASH. The results support a model in which during the development of NASH, lipotoxicity triggers caspase 3 activation in hepatocytes, resulting in hepatocellular damage and steatohepatitis development. Caspase 3 activation further induces the release of signals that activates HSC resulting in fibrogenesis and eventually fibrosis. These data have significant implications for development of potential targets for therapeutic intervention.

Acknowledgments This work was supported by NIH Grants (DK076852) and (DK082451) to AEF.

Conflict of interest None.

References

- Wieckowska A, Feldstein AE. Nonalcoholic fatty liver disease in the pediatric population: a review. *Curr Opin Pediatr*. 2005;17:636–641.
- Angulo P. Nonalcoholic fatty liver disease. *N Engl J Med*. 2002;346:1221–1231.
- Browning JD, Szczepaniak LS, Dobbins R, et al. Prevalence of hepatic steatosis in an urban population in the United States: impact of ethnicity. *Hepatology*. 2004;40:1387–1395.
- Schwimmer JB, Deutsch R, Kahen T, Lavine JE, Stanley C, Behling C. Prevalence of fatty liver in children and adolescents. *Pediatrics*. 2006;118:1388–1393.
- Wieckowska A, Feldstein AE. Diagnosis of nonalcoholic fatty liver disease: invasive versus noninvasive. *Semin Liver Dis*. 2008;28:386–395.
- Adams LA, Lymp JF, St Sauver J, et al. The natural history of nonalcoholic fatty liver disease: a population-based cohort study. *Gastroenterology*. 2005;129:113–121.
- Matteoni CA, Younossi ZM, Gramlich T, Boparai N, Liu YC, McCullough AJ. Nonalcoholic fatty liver disease: a spectrum of clinical and pathological severity. *Gastroenterology*. 1999;116:1413–1419.
- Ekstedt M, Franzen LE, Mathiesen UL, et al. Long-term follow-up of patients with NAFLD and elevated liver enzymes. *Hepatology*. 2006;44:865–873.
- Feldstein AE, Canbay A, Angulo P, et al. Hepatocyte apoptosis and fas expression are prominent features of human nonalcoholic steatohepatitis. *Gastroenterology*. 2003;125:437–443.
- Cazanave SC, Gores GJ. Mechanisms and clinical implications of hepatocyte lipoapoptosis. *Clin Lipidol*. 2010;5:71–85.
- Li J, Yuan J. Caspases in apoptosis and beyond. *Oncogene*. 2008;27:6194–6206.
- Weber IT, Fang B, Agniswamy J. Caspases: structure-guided design of drugs to control cell death. *Mini Rev Med*. 2008;8:1154–1162.
- Pop C, Salvesen GS. Human caspases: activation, specificity, and regulation. *J Biol Chem*. 2009;284:21777–21781.
- Earnshaw WC, Martins LM, Kaufmann SH. Mammalian caspases: structure, activation, substrates, and functions during apoptosis. *Annu Rev Biochem*. 1999;68:383–424.
- Fuentes-Prior P, Salvesen GS. The protein structures that shape caspase activity, specificity, activation and inhibition. *Biochem J*. 2004;384:201–232.
- Feldstein A, Gores GJ. Steatohepatitis and apoptosis: therapeutic implications. *Am J Gastroenterol*. 2004;99:1718–1719.
- Wieckowska A, Zein NN, Yerian LM, Lopez AR, McCullough AJ, Feldstein AE. In vivo assessment of liver cell apoptosis as a novel biomarker of disease severity in nonalcoholic fatty liver disease. *Hepatology*. 2006;44:27–33.
- Hatting M, Zhao G, Schumacher F, et al. Hepatocyte caspase-8 is an essential modulator of steatohepatitis in rodents. *Hepatology*. 2013;57:2189–2201.
- Dixon LJ, Flask CA, Papouchado BG, Feldstein AE, Nagy LE. Caspase-1 as a central regulator of high fat diet-induced nonalcoholic steatohepatitis. *PLoS One*. 2013;8:e56100.
- Woo M, Hakem R, Soengas MS, et al. Essential contribution of caspase 3/CPP32 to apoptosis and its associated nuclear changes. *Genes Dev*. 1998;12:806–819.
- Nanji AA. Animal models of nonalcoholic fatty liver disease and steatohepatitis. *Clinics in Liver Disease*. 2004;8:559–574, ix.
- Koteish A, Diehl AM. Animal models of steatosis. *Semin Liver Dis*. 2001;21:89–104.
- Kleiner DE, Brunt EM, Van Natta M, et al. Design and validation of a histological scoring system for nonalcoholic fatty liver disease. *Hepatology*. 2005;41:1313–1321.
- Alkhoury N, Dixon LJ, Feldstein AE. Lipotoxicity in nonalcoholic fatty liver disease: not all lipids are created equal. *Expert Rev Gastroenterol Hepatol*. 2009;3:445–451.
- Feldstein AE, Gores GJ. Apoptosis in alcoholic and nonalcoholic steatohepatitis. *Front Biosci*. 2005;10:3093–3099.
- Li Z, Berk M, McIntyre TM, Gores GJ, Feldstein AE. The lysosomal-mitochondrial axis in free fatty acid-induced hepatic lipotoxicity. *Hepatology*. 2008;47:1495–1503.
- Feldstein AE, Canbay A, Guicciardi ME, Higuchi H, Bronk SF, Gores GJ. Diet associated hepatic steatosis sensitizes to Fas mediated liver injury in mice. *J Hepatol*. 2003;39:978–983.
- Feldstein AE, Werneburg NW, Canbay A, et al. Free fatty acids promote hepatic lipotoxicity by stimulating TNF- α expression via a lysosomal pathway. *Hepatology*. 2004;40:185–194.
- Green DR. Apoptotic pathways: ten minutes to dead. *Cell*. 2005;121:671–674.
- Chowdhury I, Tharakan B, Bhat GK. Caspases—an update. *Comp Biochem Physiol B Biochem Mol Biol*. 2008;151:10–27.
- Barreyro FJ, Holod S, Finocchietto PV et al. The pan-caspase inhibitor emricasan (IDN-6556) decreases liver injury and

- fibrosis in a murine model of non-alcoholic steatohepatitis. *Liver Int.* 2014. (Epub ahead of print). doi:10.1111/liv.12570.
32. Witek RP, Stone WC, Karaca FG, et al. Pan-caspase inhibitor VX-166 reduces fibrosis in an animal model of nonalcoholic steatohepatitis. *Hepatology.* 2009;50:1421–1430.
 33. Anstee QM, Concas D, Kudo H, et al. Impact of pan-caspase inhibition in animal models of established steatosis and non-alcoholic steatohepatitis. *J Hepatol.* 2010;53:542–550.
 34. Alkhoury N, Gornicka A, Berk MP, et al. Adipocyte apoptosis, a link between obesity, insulin resistance, and hepatic steatosis. *J Biol Chem.* 2010;285:3428–3438.
 35. Syn WK, Choi SS, Diehl AM. Apoptosis and cytokines in non-alcoholic steatohepatitis. *Clin Liver Dis.* 2009;13:565–580.
 36. Imamura M, Ogawa T, Sasaguri Y, Chayama K, Ueno H. Suppression of macrophage infiltration inhibits activation of hepatic stellate cells and liver fibrogenesis in rats. *Gastroenterology.* 2005;128:138–146.
 37. Seki E, De Minicis S, Gwak GY, et al. CCR1 and CCR5 promote hepatic fibrosis in mice. *J Clin Investig.* 2009;119:1858–1870.
 38. Tacke F. Functional role of intrahepatic monocyte subsets for the progression of liver inflammation and liver fibrosis in vivo. *Fibrogenesis Tissue Repair.* 2012;5:S27.
 39. Karlmark KR, Weiskirchen R, Zimmermann HW, et al. Hepatic recruitment of the inflammatory Gr1 + monocyte subset upon liver injury promotes hepatic fibrosis. *Hepatology.* 2009;50:261–274.
 40. Seki E, de Minicis S, Inokuchi S, et al. CCR2 promotes hepatic fibrosis in mice. *Hepatology.* 2009;50:185–197.